17th World Conference on Earthquake Engineering, 17WCEE
Sendai, Japan - September 13th to 18th 2020

LOAD-BEARING PROPERTIES OF STEEL BRIDGE PIERS SUBJECTED TO MULTIPLE CONSECUTIVE STRONG MOTIONS

T. Kitahara[(1)], R. Sudoh[(2)], and Y. Ohtani[(3)]

[(1)] *Prof., Kanto Gakuin University, kitahara@kanto-gakuin.ac.jp*
[(2)] *Graduate student, Kanto Gakuin University, m18j4007@kanto-gakuin.ac.jp*
[(3)] *Assistant., Kanto Gakuin University, ohtani@kanto-gakuin.ac.jp*

Abstract

In the 2016 Kumamoto earthquake in Japan, strong ground motions occurred consecutive within a few days. According to the Japan Meteorological Agency, earthquakes with JMA seismic intensity of 6- or more were observed 7 times and earthquakes with JMA seismic intensity of 5+ or more were observed 12 times. When multiple consecutive strong earthquakes occur, the structure damaged by the first earthquake will again undergo amplitude reaching the plastic zone. This problem is an important issue, but few previous studies have been done, so seismic performances of structures subjected to multiple consecutive waves are not clear. In seismic design codes in many countries, there are no specific descriptions concerned with the seismic performance of structure subjected to such input motions. This study evaluated load-bearing characteristics of existing steel bridge piers by complex non-liner (geometric nonlinearity and material nonlinearity) Finite Element Analyses using static cyclic-load simulating multiple sequential strong motions. In numerical calculation, 3 target steel piers with the different of width-thickness ratio parameter and slenderness ratio parameter as buckling parameter were prepared. These piers were the simple box type cross-section without ribs and the width-thickness ratio parameter were 0.5, 0.55, and 0.6. Moreover, 2 target steel piers with the different of diameter-thickness ratio parameter were prepared. These piers were the pipe type cross-section without ribs and the diameter-thickness ratio parameter were 0.075, and 0.100. As a result, it is found that the load-bearing capacity decreases with cyclic loading as the buckling parameter is larger and the number of loading in each cycle is larger. These capacity decreasing is occur due to the progress of local buckling of steel piers.

Keywords: consecutive strong motion; load-bearing properties; deterioration; steel bridge pier; non-linear FEM

1. Introduction

During 2016 Kumamoto Earthquake in Japan, severe ground motions with JMA seismic intensity of 7 were observed two times within a few days. Also, many strong seismic motions were measured (7 times were larger than JMA seismic intensity of lower 6 and 12 times were larger than higher 5). Due to such consecutive strong motions, structures damaged by first earthquake may perform plastic behavior again by later earthquakes and decrease its load-bearing capacity. In seismic design codes in Japan [1] and other many countries [2, 3], there are no specific descriptions about seismic performance of structures subjected to multiple consecutive waves and few previous studies about this issue have been done.

Recently, decrease of load-bearing capacity of steel piers due to subduction-zone type long time duration earthquake, e.g. 2011 Great East Japan Earthquake was studied [4, 5]. It was found that load-bearing capacity would decrease as the progress of local buckling by cyclic-loads within elastic range after maximum strength, and buckling parameters e.g. width-thickness ratios strongly effect on the degree of deterioration. Also, the effects of two different types of constitutive model (kinematic hardening type bilinear model and modified two surface model) on deterioration was studied [6]. It was found that modified 2 surface model had better accuracy with experimental results.

In this paper, load-bearing characteristics of existing steel piers are studied by complex non-linear (geometric nonlinearity and material nonlinearity) Finite Element analysis using static cyclic-loadings as multiple consecutive strong motions. In addition to loading conditions corresponding to the situation that strong motion with same amplitude occurs three times in a row, the effects of intensity reduction in aftershock and difference of duration time are also considered.

2. Analytical model

In this paper, complex non-linear (geometric nonlinearity and material nonlinearity) Finite Element analysis is performed using FEM software (DIANA).

Fig. 1 shows analytical model of existing steel piers used on highway bridges. Target piers are thin-walled box cross-section without ribs, and modelled by curved shell elements divided into seven sections in plate thickness direction. Initial imperfections (initial deflection and residual stress) are not considered. Three target piers have different width-thickness ratio parameter (R_f = 0.5, 0.55 and 0.6) and fixed slenderness ratio parameter (λ = 0.35) [7, 8]. Considering the current design standard [1], the width-thickness ratio parameter (R_f = 0.6) is slightly larger. However, this study was performed using the width-thickness ratio paramerer which has a large effect on local buckling, because the existing bridge piers are targeted.

Table 1-2 shows structural properties and material properties. Material nonlinearity is modeled as kinematic hardening type bilinear model to clarify the elasto-plastic properties of steel that experiences sequential strong motions. Yield condition is modelled as von-Mises plastic model and second stiffness is represented by E/100.

$$R_f = \frac{b}{t}\sqrt{\frac{\sigma_y}{E}\frac{12(1-\mu^2)}{k\pi^2}} \tag{1}$$

$$\bar{\lambda} = \frac{1}{\pi}\sqrt{\frac{\sigma_y}{E}}\frac{\ell}{r} \tag{2}$$

where b : width of flange, t : diameter, σ_y : yield stress od steel, E : young's modulus, υ : poisson's ratio, k : buckling coefficient, l : buckling length.

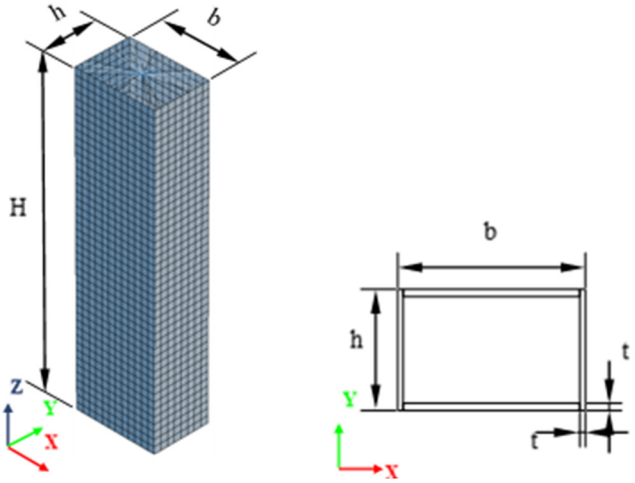

(a) Overall view (b) Cross-sectional shape

Fig. 1 – Analytical model

Table 1 – Structural properties

Analytical model	A	B	C
Height H (mm)	681	669	612
Flange width b (mm)	184	168	154
Web width h (mm)	122	112	102
Thickness t (mm)	6.5	6.5	6.5
Width-thickness ratio parameter R_f	0.60	0.55	0.50
Slenderness ratio parameter λ	0.35	0.35	0.35
Yield bending moment M_y (kN·m)	45.7	43.8	36.5
Yield horizontal Load H_y (kN)	67.1	65.4	59.6
Yield horizontal displacement δ (mm)	3.65	3.84	3.53

Table 2 – Material properties

Young modulus E (kN/mm^2)	Poisson ratio ν	Density ρ(kg/mm^3)
206	0.273	7.7

3. Loading condition

As the initial condition, the axial force corresponding to mass of superstructure acts on the center node of upper surface in z-direction. This node is connected to each node at upper end of shell elements as rigid element. After that, forced displacement representing horizontal displacement of piers acts on same node in y-direction.

Table 3 shows loading conditions of forced displacement. Every case has three loading cycles corresponding to the situation that strong motion with same amplitude occurs three times in a row. Also, each case has two subcases to consider the difference of duration time. One is the case that forced displacement with same amplitude is repeated three times in each loading cycle and the other is the case that same amplitude is repeated two times. Fig. 2 shows loading cases for model $R_f = 0.60$.

Table 3 – Loading conditions

Case	Repeated time of Same Amplitude	Maximum Amplitude of Forced Displacement	Decrease of Input Intensity
A-2	2	Corresponds to 90% of Maximum Bearing Force	Not Considered
A-3	3		
B-2	2		Considered
B-3	3		
C-2	2	Corresponds to maximum bearing force	Not Considered
C-3	3		
D-2	2		Considered
D-3	3		

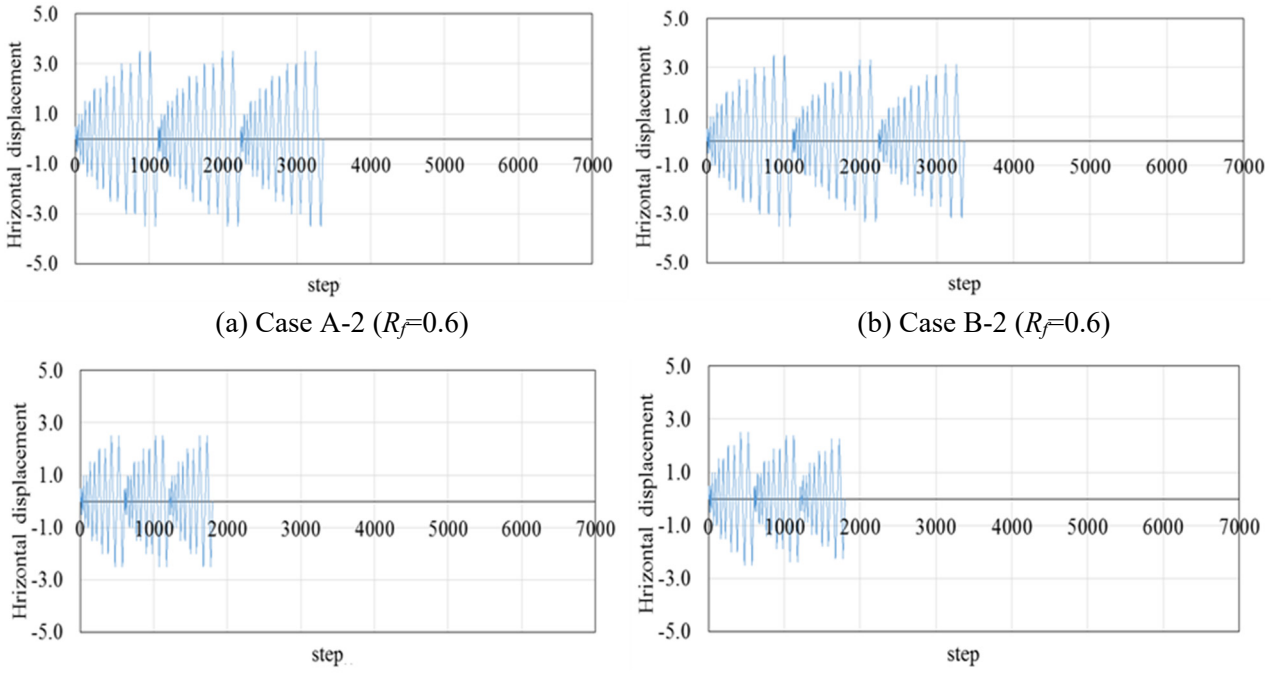

(a) Case A-2 (R_f=0.6) (b) Case B-2 (R_f=0.6)

(c) Case C-2 (R_f=0.6) (d) Case D-2 (R_f=0.6)

Fig. 2 – Loading conditions

In case A, maximum amplitude of horizontal displacement at each loading cycle corresponds to 90% of maximum strength after local buckling occurs and the model experiences maximum bearing force. This case represents the situation that strong motion with same amplitude occurs three times in a row. Horizontal displacement is $\delta/\delta_y = 3.5, 3.5, 4.0$ when $R_f = 0.60, 0.55, 0.50$, respectively.

In case B, maximum amplitude of horizontal displacement at first loading cycle corresponds to 90% of maximum load after the model experiences maximum bearing force. Also, maximum amplitude of second and

third cycles is 0.95 times and 0.9 times larger than that of first cycle, respectively. This case represents the situation that after shock with smaller intensity than main shock occurs two times in a row.

In case C, maximum amplitude of each loading cycle corresponds to maximum bearing force. Horizontal displacement is $\delta/\delta_y = 2.5$.

In case D, maximum amplitude of each loading cycle corresponds to maximum bearing force and maximum amplitude of second and third cycle is 0.95 times and 0.90 times larger than that of first cycle, respectively.

4. Analytical results and discussions

Fig. 3-5 shows horizontal force-displacement relationships of A-2, B-2, C-2 and D-2. In these figures, forces and displacements are normalized by the values at yield. Each figure shows the differences based on the decrease of input intensity.

In these figures, only the results for the case with 2 repetitions are shown. Because the horizontal force-displacement relation shows same tendency regardless of the repetition number of same displacement amplitude at each loading cycle. It can be seen that there are almost no differences in force-displacement relationship between case A and C or B and D within horizontal displacement δ/δ_y is smaller than 2.5, however load-bearing capacity decreases as δ/δ_y becomes larger than 2.5 because of the progress of local buckling.

Figure 6 shows the relationship between deterioration ratio of strength and number of cycle for each case. Deterioration ratio is defined at each step with maximum displacement amplitude as the difference from initial maximum loading. Only the deterioration ratio at last step of each loading cycle is shown in the figure. It can be seen that load-bearing capacity decreases more than 9.5% at first cycle and around 15-16% at third cycle in case A and C because of the progress of local buckling.

On the other hand, load-bearing capacity decreases less than 1% at first cycle and around 3-6% at third cycle in case B and D. Also, load-bearing capacity decreases as width-thickness ratio becomes larger but the difference is not so much in case A and B. It is also necessary to consider a smaller width-thickness ratio.

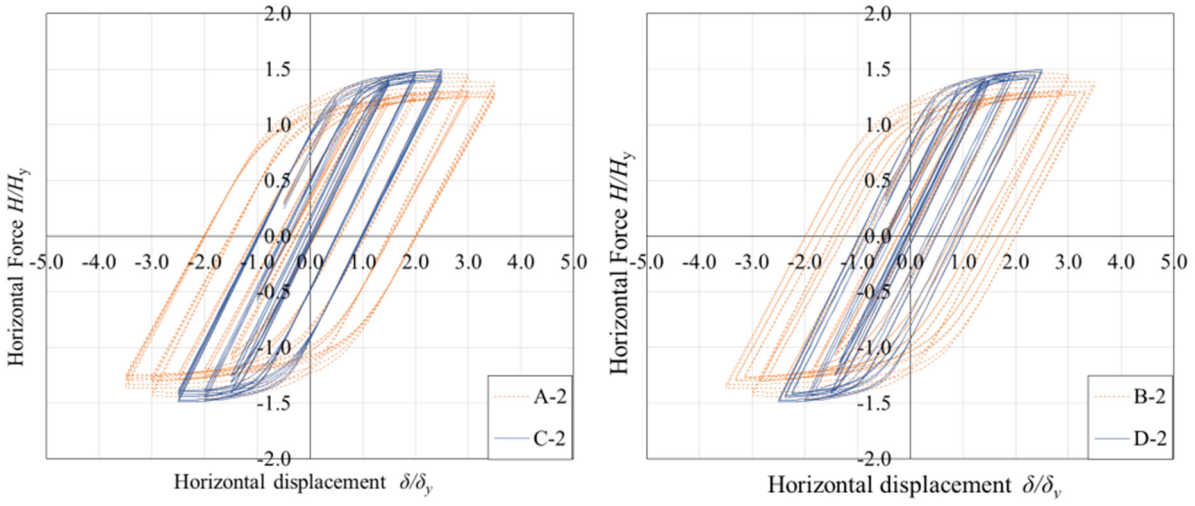

(a) Case A and C (b) Case B and D

Fig. 3 – Load-bearing relationship (R_f=0.6)

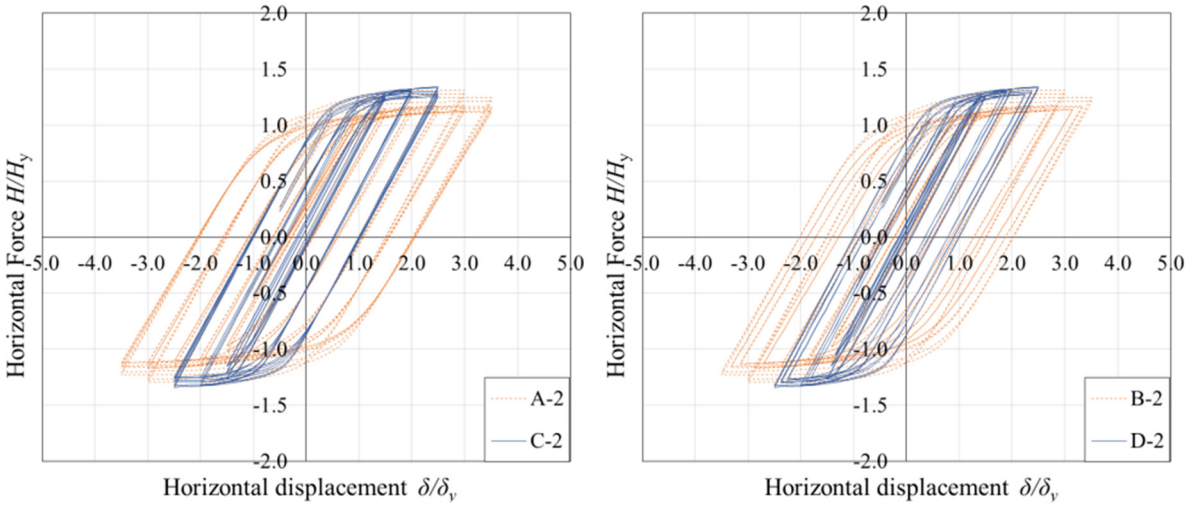

(a) Case A and C (b) Case B and D

Fig. 4 – Load-bearing relationship (R_f=0.6)

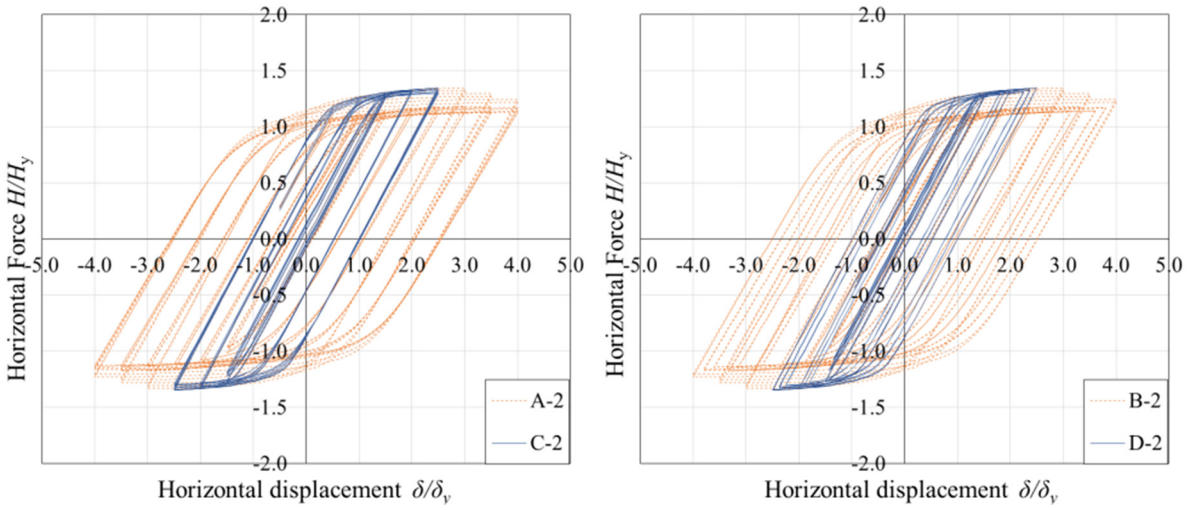

(a) Case A and C (b) Case B and D

Fig. 5 – Load-bearing relationship (R_f=0.6)

Figure 7 shows the bottom deformation of R_f= 0.6 model at the end of cyclic loading. The deformation magnification is shown as 5 times. It can be seen that concave local buckling occurs on the flange and convex local buckling occurs on the web. It has been confirmed that this local buckling progresses due to the continuously input strong motions. This progress of local buckling is one of the reason why the bearing capacities of bridge piers is decreasing due to cyclic loading.

5. Conclusions

We performed nonlinear Finite Element analysis for existing steel piers subjected to multiple consecutive strong motions such as 2016 Kumamoto Earthquake.

We showed the tendency of load-bearing capacity due to the difference of buckling parameters. In this study, it is found that the load-bearing capacity decreases about 10% at first cycle and more than 15% at third cycle by forced displacement with the amplitude which corresponds to maximum bearing force obtained from

pushu-over analysis. We think it seems necessary to consider the effect of these degradation of load-bearing capacity in seismic design and reinforcement.

We will plan to consider in detail about the effect of loading condition as multiple consecutive strong motions in future work.

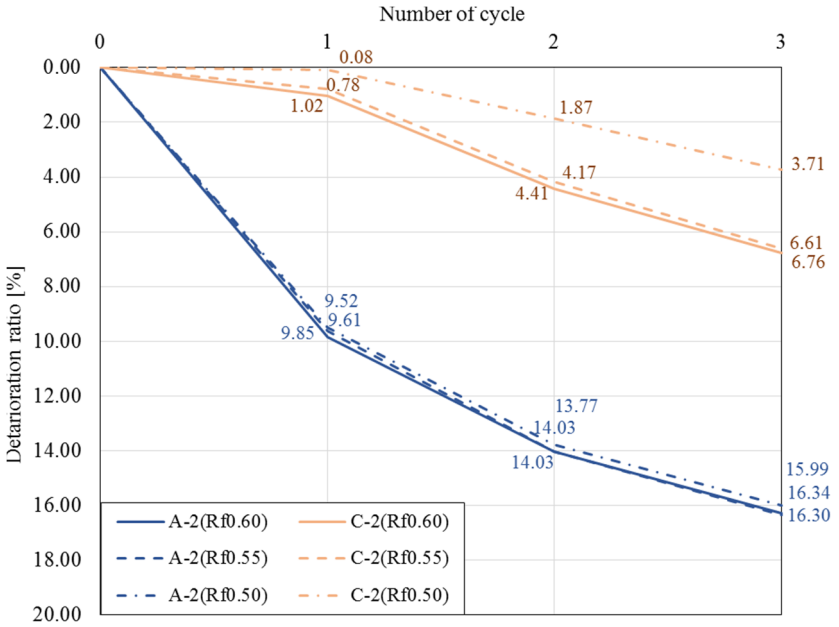

(a) Comparison of Case A and C

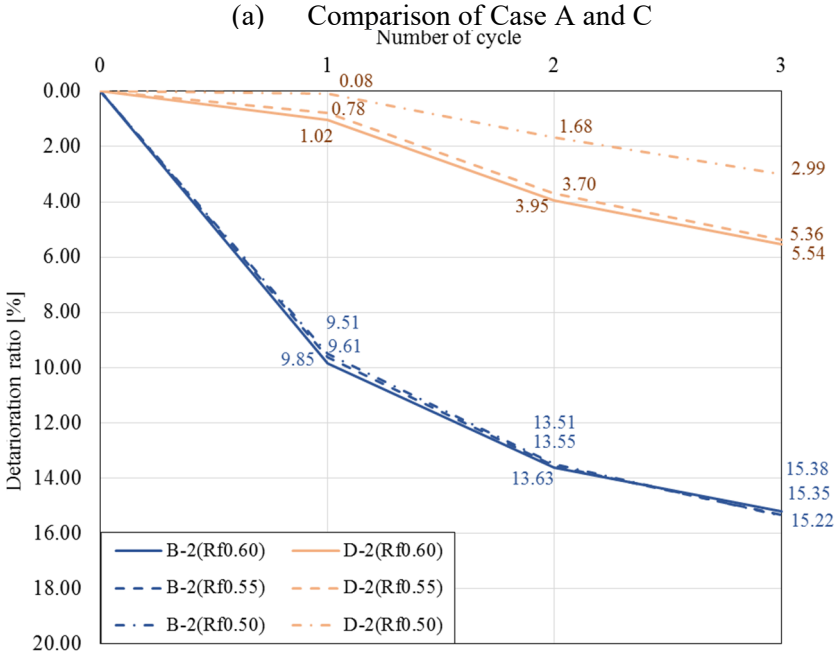

(b) Comparison of Case B and D

Fig. 6 – Deterioration ratio of strength

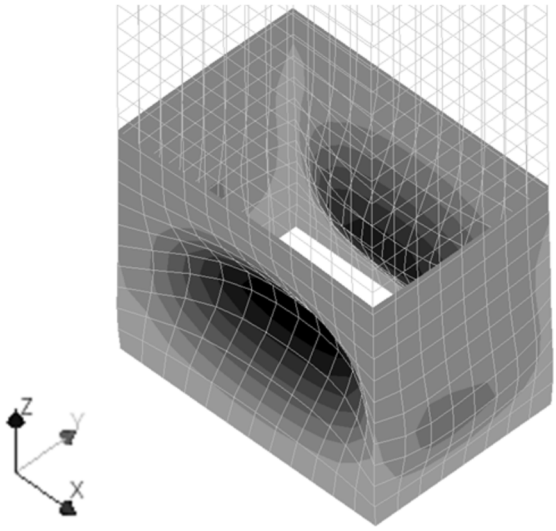

Fig. 7 – Deformation at bridge pier bottom

Acknowledgements

This research was carried out as a part of JP18K04332 and JP17H03297.

References

[1] Japan Road Association (2016): *Specifications for Highway Bridges Part V Seismic Design*, Maruzen, 2012 English version.

[2] State of California Department of transportation (2019): *Caltrans Seismic Design Criteria*, Caltrans, Version 2.0.

[3] NZ transport Agency (2018): *Bridge Manual,* 3rd edition.

[4] Kitahara T, Tanaka K, Yamaguchi T (2010): Load Bearing Capacities of Steel Bridge Piers Subjected to Long-duration Time Motions, *9th US national and 10th Canadian Conference on Earthquake Engineering*, Toronto, Canada.

[5] Kitahara T, Kishi Y, Ohtani Y (2015): Strength deterioration of Steel bridge piers subjected to long duration time motions, *10th pacific Conference on Earthquake Engineering*, Sydney, Australia.

[6] Kitahara T, Ohtnai Y, Kishi Y, Kasai A (2016): Load-bearing properties of steel bridge piers subjected to consecutive strong motions and long duration time motions, *19th Symposium on Performance-based Seismic Design Method for Bridges*, Tokyo, Japan (in Japanese).

[7] Shen, C, Mizuno, E, Usami, T (1993): A Generalized Two-surface Model for Structural Steels under Cyclic Loading, *Structural Engineering/Earthquake Engineering,* **10** (2), 59-69.

[8] Japan Road Association (2017): *Specifications for Highway Bridges Part II Steel Bridges*, Maruzen, 2012 English version.

